Research on Engineering Structures & Materials

journal homepage: http://www.jresm.org

Research Group

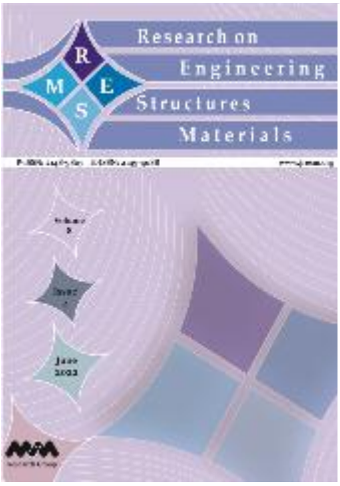

Effect of blowing ratio on adiabatic effectiveness for effusion cooling in gas turbine combustor liners

KR Yellu Kumar, Adnan Qayoum, Shahid Saleem, Fasil Qayoom Mir

Online Publication Date: 15 Mar 2022

URL: http://www.jresm.org/archive/resm2022.359me1028.html

DOI: http://dx.doi.org/10.17515/resm2022.359me1028

Journal Abbreviation: *Res. Eng. Struct. Mater.*

To cite this article

Kumar KRY, Qayoum A, Saleem S, Mir FQ. Effect of blowing ratio on adiabatic effectiveness for effusion cooling in gas turbine combustor liners. *Res. Eng. Struct. Mater.*, 2022; 8(3): 431-445.

Research on Engineering Structures & Materials
journal homepage: http://www.jresm.org
MIM Research Group

Research Article

Effect of blowing ratio on adiabatic effectiveness for effusion cooling in gas turbine combustor liners

KR Yellu Kumar[1,a], Adnan Qayoum[*1,b], Shahid Saleem[1,c], Fasil Qayoom Mir[2,d]

[1]*Mechanical Engineering Department, National Institute of Technology Srinagar, J&K, India-190006.*
[2]*Chemical Engineering Department, National Institute of Technology Srinagar, J&K, India-190006*

Article Info

Article history:
Received 28 Oct 2021
Revised 14 Feb 2022
Accepted 11 Mar 2022

Keywords:

Effusion cooling; Adiabatic effectiveness; Blowing ratio; Injection angle; Combustor liners; Gas turbine

Abstract

The current study involves a computational investigation on the cooling of the combustion chamber liners in a gas turbine engine. Effusion cooling is a high-efficiency, lightweight and low-cost cooling system widely used in combustion chamber liners nowadays. The effect of blowing ratio and effusion hole injection angle on adiabatic effectiveness is investigated. The simulations are carried using COMSOL Multiphysics 5.4 with the standard k- ε turbulence model. A 3D computational model consisting of mainstream duct, effusion plate and effusion holes has been incorporated for the analysis. The blowing ratios used in the study are 0.25, 0.5, 1, 1.25 and 1.5 at constant density ratio of 1.0 for different injection angles of 30° and 60°. The simulation results show a strong dependence of adiabatic effectiveness on the blowing ratios. For low blowing ratios the adiabatic effectiveness in effusion hole region is high on account of coolant being attached to the surface. On the contrary, for high blowing ratios the adiabatic effectiveness is low near the effusion holes region. In the downstream region of effusion holes the adiabatic effectiveness raises for high blowing ratios. In addition, it has been observed that injection angle of 30° provides better adiabatic effectiveness compared to injection angle of 60°. The velocity and temperature profiles are investigated to demonstrate the behavior of coolant flow on the effusion surface and the influence on adiabatic effectiveness. This study concludes that the proper selection of blowing ratio and injection angle improves combustion chamber's efficiency and lifetime.

1. Introduction

To achieve the high thermal efficiency of a gas turbine or aero engines the turbine inlet temperatures are maintained around 1200°C-1500°C [1-4] which is clearly above the metallurgical limit of the metals. As a consequence, cooling has to be initiated to avoid local thermal cracks and reduces the chances of failure. A proper cooling method should be introduced on the hot sections of gas turbines such as combustion chamber, turbine blades, and nozzle to enhance their operational life. However, to follow the strict emission legislation it is mandatory to maintain the NO_x and CO levels within the permissible limits. Coolant consumption plays a vital role in the design aspect of a cooling system which is a key point to increase the cycle efficiency and utilization of lean burn mixture combustion. This will automatically ensure NO_x reduction to fulfill the emission legislation.

Compared to other cooling techniques, effusion cooling is considered as most advanced cooling concept in which the coolant or secondary flow is injected through an array of closely spaced holes or slots which enters the thermal boundary layer of combustion liners

*Corresponding author: adnan@nitsri.ac.in
[a] orcid.org/0000-0001-9793-7577; [b] orcid.org/0000-0002-4894-3425; [c] orcid.org/0000-0001-6998-0324; [d] orcid.org/0000-0002-3211-2395
DOI: http://dx.doi.org/10.17515/resm2022.359me1028

resulting in the formation of film. This film serves as the protection layer between the hot gases and wall surface. Effusion cooling involves injection of air through holes whose size and number may vary. The hole density on the surface increases as large number of holes is arranged at very close spacing in arrays. Due to this, coalescence of adjacent jet increases by increasing the overall cooling performance on the surface. Effusion cooling involves two heat exchange effects, the first one being the convective cooling inside the wall as the coolant passes through the holes and other is the formation of coolant film on the wall as coolant passes over the wall surface. Since last two decades researchers have focused on the improvement of effusion cooling performance due to its simplicity and reliability for providing continuous cooling over the hot sections of gas turbine. Due to high fabrication cost and challenging technical issues, it is difficult to carry out experimentation for the complete combustion chamber. Numerical studies provide an important complimentary design tool and refine overall results due to availability of advanced computational fluid dynamics. Still experimentation is carried out on a flat plate with drilled holes similar to real as combustion liners a set up similar to the conventional wind tunnel. Considering the past literature review, it is observed that both geometrical and flow parameters such as hole shape, hole diameter, hole injection angle, blowing ratio, density ratio and thermal conductivity etc., have a strong influence on the effusion cooling performance. Yuen and Matinez [1] studied the effect of hole injection angle (α) by measuring adiabatic effectiveness and heat transfer coefficient on a flat plate with various geometries for different blowing ratios ranging from 0.33 to 2.0. Roger and Buck [5] concluded that the use of the k-ε turbulence model generates better data that were close to the predicted results, Lamyaa and Deborah [6] compared the standard k-ε turbulence model with Yang-Shih turbulence model for cross-flow conditions through angled holes with the experimental results. Silieti et al. [7] computationally investigated film cooling over flat surface using five turbulence model; the standard k-ε model, the realizable k-ε model, the RNG k-ε model, the standard k-ω model and the SST k- ω model. He concluded that the standard k-ε turbulence model predicted close conformity to the experimental results for the center line adiabatic effectiveness in the downstream region. Baldauf et al. [8] investigated experimentally and measured the laterally averaged adiabatic effectiveness (η) over a flat plate at different blowing ratios and found that the value of η increases first and then decreases. This is on account of overshooting into the mainstream flow by detaching the coolant flow from the surface. Ligrani et al. [9] measured the heat transfer coefficient and adiabatic effectiveness for effusion cooling system by studying the impact of blowing ratio and spacing of coolant holes over the adiabatic effectiveness.

Bailey et al. [11] investigated the heat transfer characteristics of impingement cooling for a stationary combustor comprising of trip strip tabulators for enhancement of heat transfer and studied the distribution of heat transfer coefficient over the flat plate by using steady state liquid crystal method. Investigations on effusion cooling performance were examined by Liu and Zheng [12] on four deflection angles and it was observed that cooling performance decrease after the primary holes due to the local combustion. The authors used 3D fluid-solid coupling to measure the effusion cooling performance. Andrew et al. [13-15] performed number of experiments to study the geometrical parameter effects such as cooling hole shape, hole diameter and hole injection angle. The authors [16-17] investigated both experimentally and numerically to study the pitch-to-pitch hole spacing in streamwise and spanwise direction, different hole injection angles and deflection angles by measuring the adiabatic film effectiveness at different blowing ratios. Legar et al. [18] examined the effect of pressure difference between the hot and cold gas for effusion cooling system with different geometry and flow parameters. They conducted experimentation in temperature range of 860K-1400K similar to a real combustor condition. From their observations they suggested two zones system for effusion cooling which can improve the cooling performance by reducing the coolant mass flow rate.

Gaustafsson [19] explained the effect of blowing ratio and temperature ratio on effusion cooling performance over a flat plate surface. Sasaki et al. [20] conducted experiments on staggered manner arrangement with spacing of holes in streamwise direction $S_x/d=10$ and $S_y/d=3$ at injection angles $\alpha=45^o$. They observed that array arrangement increases the lateral averaged effectiveness by increasing the blowing ratio than single row of holes. Cerri et al. [21] studied the effect of hole diameter and spacing of holes in streamwise direction (S_x/d) and (S_y/d) and suggested that an efficient cooling system can be achieved only by reducing the mass coolant flow consumption. Yellu et al. [22] has compiled a comprehensive review of effusion cooling in Gas turbine combustion chamber. The study shows a significant dependence of various parameters on the adiabatic efficiency.

The objective of this paper is to evaluate the adiabatic effectiveness of the effusion cooling plate with the purpose to study the effect of blowing ratio in the effusion holes region and downstream the effusion holes region at different injection angles. To characterize the effect of blowing ratio, a range of blowing ratios 0.25 to 1.5 with low and high values are used for the purpose. In addition, velocity and temperature profiles have been evaluated at a specified location in the streamwise direction for comprehensive understanding of the flow field.

2. Computational Model

The computational model and details of the effusion plate with inclined holes are shown in Fig. 1 and Fig. 2 respectively. The three-dimensional computational domain consists of three sub-sections i.e., mainstream flow zone, coolant flow zone and effusion plate zone. The mainstream flow (hot gases) passes over the effusion plate surface while cold stream (cool air) flows through the inclined effusion holes towards the effusion surface. The holes are arranged in staggered manner with first row located at 23d for an injection angle of 30^o and 18d for an angle of 60^o. The height of the mainstream flow duct is 30d (in Z-direction) and the corresponding width (in Y-direction) is twice the spanwise distance between the adjacent holes (see Fig. 2). The symmetric boundary conditions are applied on either side of domain. In order to understand, the temperature distribution over the surface in streamwise direction the mainstream flow domain is divided in three zones i.e., upstream region (X_1), effusion holes region (X_2) and downstream region (X_3). The coolant flow holes are present in the effusion holes region (X_2) only. The geometrical parameters of the effusion plate are shown in Table 1.

Table 1. The geometry parameters of the effusion plate are

d	1 mm
t	3 mm
S_x/d	4.9
S_y/d	4.9
α	30° and 60°

3. Boundary Conditions

Air is modelled as incompressible for both mainstream and coolant. The primary inlet of hot gas is set to specified velocity while the outlet is set to static pressure conditions. Inlet velocity of mainstream flow is fixed at a specified velocity $U_\infty=50$ m/s and coolant velocities are varied to study the effect of BR for different cases i.e., 0.25, 0.5, 1, 1.25 and 1.5. The inlet temperatures for mainstream and coolant flow are fixed at $T_\infty=350$K and $T_c=300$ K respectively resulting in the density ratio (DR) approximately equal to one. The turbulence intensity for both inlets is specified as 5%. The properties of air such as ratio of specific heats, dynamic viscosity, heat capacity at constant pressure and thermal conductivity are dependent on the temperature. The effusion plate is set to adiabatic noslip condition with the interface between the primary flow and perforated plate as fluid-solid coupled boundary. To evaluate the adiabatic effectiveness the plate is assumed to be adiabatic. In this study adiabatic effectiveness is measured along centerline of the effusion as shown in Fig. 2

Velocity ratio (VR) is defined as ratio of coolant flow blowing to mainstream flow blowing.

$$VR = \frac{Uc}{U\infty} \tag{1}$$

The most important parameter that affects the effusion cooling performance is Blowing ratio (BR). It is defined as the ratio of coolant mass flux to mainstream mass flux.

$$BR = \frac{\rho_c U_c}{\rho_c U_c} \tag{2}$$

The adiabatic effectiveness of effusion cooling is measured in terms of

$$\eta = \frac{T\infty - T_{wt}}{T\infty - T_c} \tag{3}$$

where T_∞, T_{wt} and T_c represents the temperatures of mainstream flow, wall temperature of effusion plate and the coolant flow respectively. In these study blowing ratios 0.25 and 0.5 are considered as low, 1.0 as intermediate, as well 1.25 and 1.5 are considered as high.

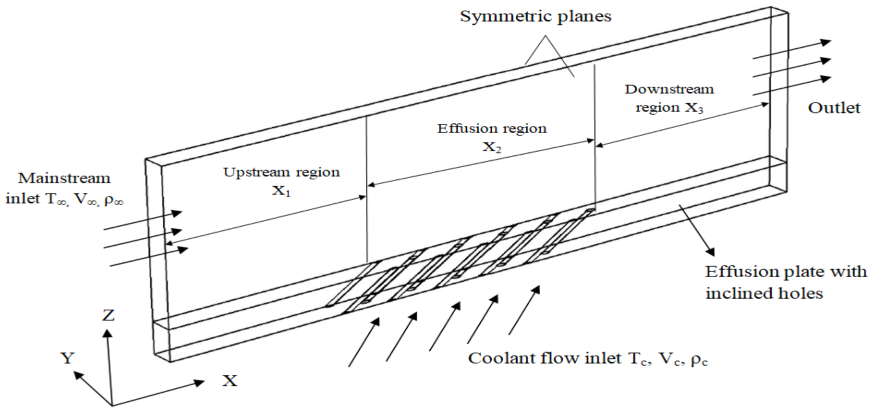

Fig. 1 Schematic of computational domain (XYZ)

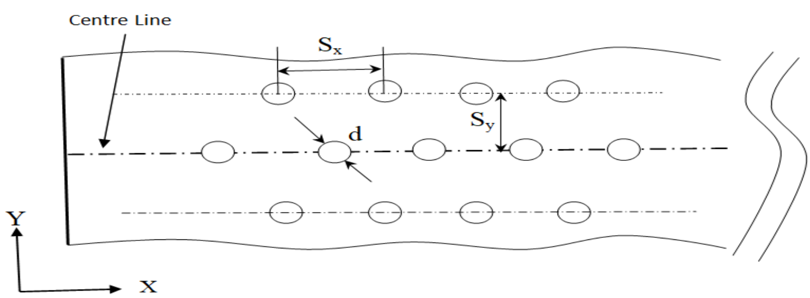

Fig. 2 Physical configuration of the problem (XY plane)

4. Computational Details

The simulations are carried using COMSOL Multiphysics 5.4 using standard k-ε turbulence model. Literature survey [5,6,7] has demonstrated that standard k-ε turbulence model can accurately predict the surface temperature distribution over the flat surface. The effectiveness of centerline film cooling can be correctly predicted by a typical k-turbulence model. User controlled mesh is used in this computational model. Free triangular mesh with extreme fine grid is chosen for the effusion plate surface and Swept mesh with fixed number of elements is distributed on the solid and fluid domain. A high resolution of grid is set near the effusion holes and effusion plate surface. At every location of the solid wall, the viscous clustering value y+ is maintained at 7. To reduce the run time of computation the symmetry in transverse planes is applied and numbers of rows of effusion holes have been reduced to 5 compared to experimental data to reduce the computational run time. The Fig. 3 shows the overall view mesh of the computational model.

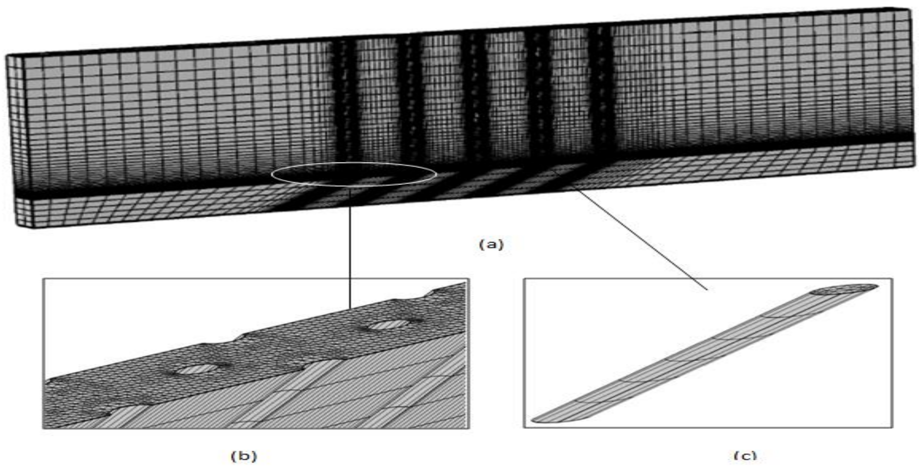

Fig. 3 Computational Mesh (a) Entire geometry (b) Effusion plate surface (c) Effusion hole

5. Grid Independence Test and Validation

The precision of numerical analysis results depends on the quality of grid used. To ensure the results obtained are independent of mesh size, the grid independence study was carried for three different grid sizes consisting of 363174 (extremely fine mesh) ,151096 (fine mesh) and 52762 (coarse mesh) elements respectively. The averaged adiabatic efficiency on the centerline of effusion surface is plotted and compared with different grids as shown in Fig. 4 for blowing ratio 0.5 at injection angle $\alpha=30^o$. The grid size of 363174 (extremely fine) is found to be quite close to the experimental results [23], with improved viewing of temperature and blowing counters on the effusion surface in the near wall region. As a result, for the final simulation, a grid size of 363174 was used. The computational results were validated by comparing with the experimental results of Scrittore et al. [23]. To validate the simulations, the same geometrical and flow parameters were used as in ref [23]. The Fig. 5 shows the comparison of experimental results and present computational results of centerline adiabatic effectiveness along the stream wise direction for 20 rows of holes at BR=3.2 and 5.0. The present results show a good agreement with the experimental data.

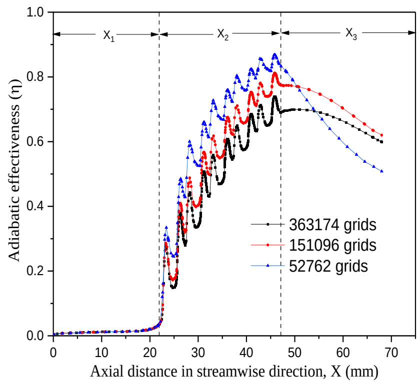

Fig. 4 Centerline adiabatic effectiveness on the effusion surface with different grid sizes for =30° and BR= 0.5

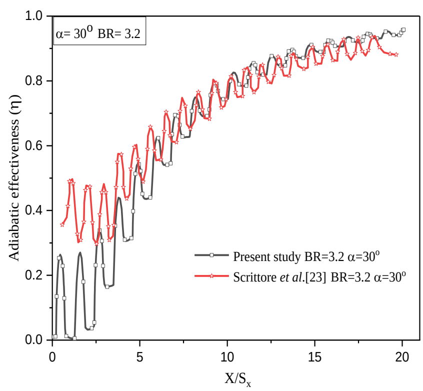

Fig. 5 Validation of experimental [23] and computational results. Note that the leading edge of first row X/S_x=0 and adiabatic effectiveness is measured from rows 1 to 20

6. Results and Discussion

The adiabatic effectiveness and temperature distribution have been calculated for all blowing ratios (BR) at two injection angles of α=30° and 60°. Since the first row of cooling holes start in the X_2 region, no heat transfer takes place before the region X_2. This is because the plate wall is considered as adiabatic and area in region X_1 shows zero effectiveness. The results included in the study are temperature distribution over the effusion plate surface and temperature slice counters on the central plane of effusion plate for different blowing ratios.

6.1 Effect of Blowing Ratio on Adiabatic Effectiveness

The Fig. 6 shows the behavior of adiabatic effectiveness (η) at different blowing ratios (BR) of 0.25, 0.5, 1, 1.25, 1.5 for injection angle (α) of 30° and 60°. The Figure clearly indicates the strong impact of blowing ratio on the adiabatic effectiveness for effusion cooling. The adiabatic effectiveness is zero in the upstream region X_1 as there is no coolant flow. In the intermediate region X_2, the adiabatic effectiveness (η) increases in the streamwise direction for all the values of the blowing ratios (BR). Further in the downstream region X_3 the adiabatic effectiveness (η) decreases at low BR (0.25 and 0.5) and increases at high BR (1, 1.25 and 1.5). On account of the low blowing ratio (BR) the coolant flow velocity is low as compared to the mainstream flow velocity so the coolant flow jet attaches to the surface without penetrating into the mainstream flow. This ensures that the hot gases do not reach the surface. At high blowing ratios (BR) the coolant jet separates from the surface by penetrating into mainstream flow and as such the hot gases reach the surface thereby increasing the surface temperature in the effusion region X_2 (see in Fig. 7 and Fig. 9). This causes the thickening of the thermal boundary layer leading to increased effectiveness. Also, it is observed from Fig. 6 that the adiabatic effectiveness (η) is high for low blowing ratio (BR) compared to that of high blowing ratios (BR) in the effusion hole region X_2. Unlike this a different behaviour is observed in the downstream region X_3. Extremely high values of adiabatic effectiveness (η) are exhibited for high blowing ratio (BR) as large amount of coolant mass flow rate is injected from effusion holes. For low blowing ratios the mass of cooling fluid injecting from effusion holes is very small and advection of mainstream gases bring hot air much closer to the wall so that the film formed over the surface become weaker as shown in Fig.7 and Fig.9. As a result, adiabatic effectiveness (η) decreases in downstream streamwise direction. But for higher blowing ratios the velocity of coolant is much higher than that of the mainstream velocity so a large amount of coolant mass flow rate is injected from the effusion holes and accumulated in the region X_3 by forming a thick film of cooling air on the surface (See in Fig. 7 and Fig 9 for high BR). This makes adiabatic effectiveness (η) high in this region at higher values of blowing ratios (see in Fig.6).

The temperature distribution on the effusion plate surface obtained for different blowing ratios (BR) at injection angles (α) of 30° and 60° are shown in Fig. 8 and Fig. 10. For lower values of blowing ratios (BR), the coolant flow remains on the surface as it does not have sufficient momentum to separate from the surface and penetrate into the mainstream flow. As such slight temperature variations can be seen as the coolant flow remains close to the surface. For higher values of blowing ratios (BR) opposite trend is observed.

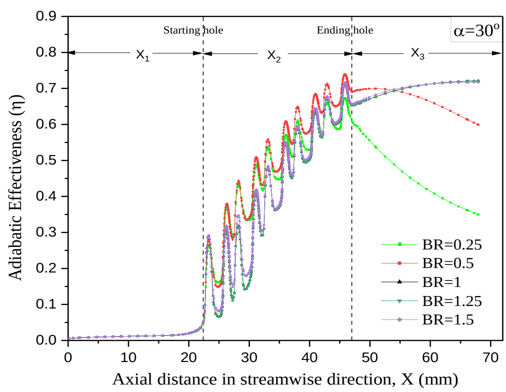

(a)

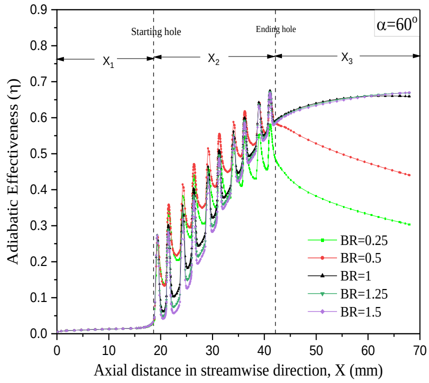

(b)

Fig. 6 Centerline adiabatic effectiveness on the surface (a) α=30° and (b) α=60°

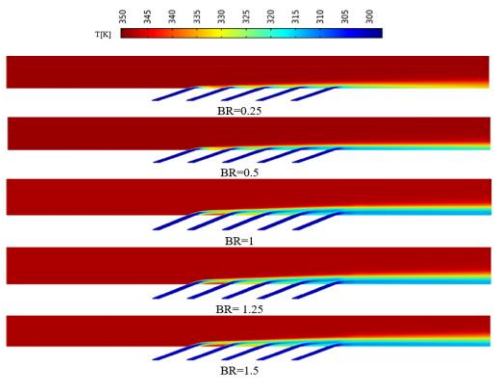

Fig. 7 Temperature slice counters on the center plane of effusion plate for different BR on XZ plane for α=30o

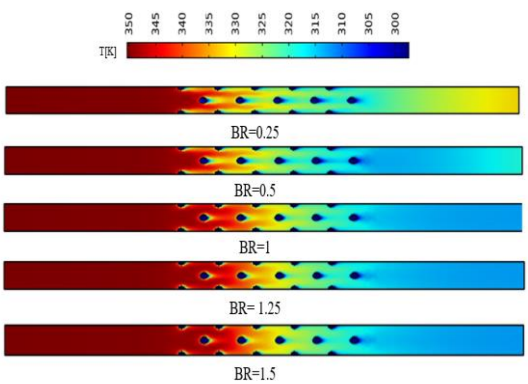

Fig.8 Temperature distribution on effusion plate surface for different BR on XY plane for α=30°

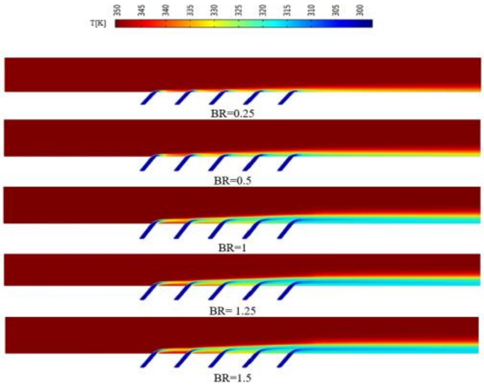

Fig.9 Temperature slice counters on the center plane of effusion plate for different BR on XZ plane for α=60°

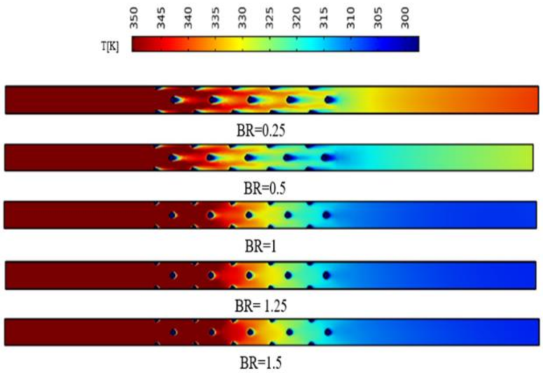

Fig.10 Temperature distribution on effusion plate surface for different BR on XY plane for α=60°

6.2 Velocity Boundary Profile

The discharged fluid from the coolant holes is mixed up with the mainstream flow in the streamwise direction and interacts with the coolant flow coming from the adjacent holes. The velocity components of the coolant jet from the effusion holes are divided into two parts, being the tangential velocity component in the streamwise direction and other being the normal velocity component in z-direction. The tangential velocity component makes the coolant to flow over the effusion wall while as the coolant flow in the normal direction penetrates into the mainstream flow. It is clear that the penetration height of the coolant flow through the effusion holes is different at various sections in streamwise direction i.e. from starting row to the ending row. Pietrzyk et al. [24] identified higher velocity fluid penetrating into wake region below the jet core causing a negative velocity gradient near the wall as such a double peaked velocity profiles can be seen in downstream of streamwise directions in the velocity profile [Fig. 11]. The double peaked velocity profiles are seen at high BR. These double peaked velocity profiles for higher value of BR are generated high due to cross flow of coolant into mainstream by the inclined jets. This is because inclined jets induce high velocity in the wake region than the normal jets on account of pressure drop and strong secondary motions. The Fig.12 shows the streamlines of mainstream flow (blue color) and coolant flow (red color) domain for blowing ratio 1.5 at injection angle 30˚.

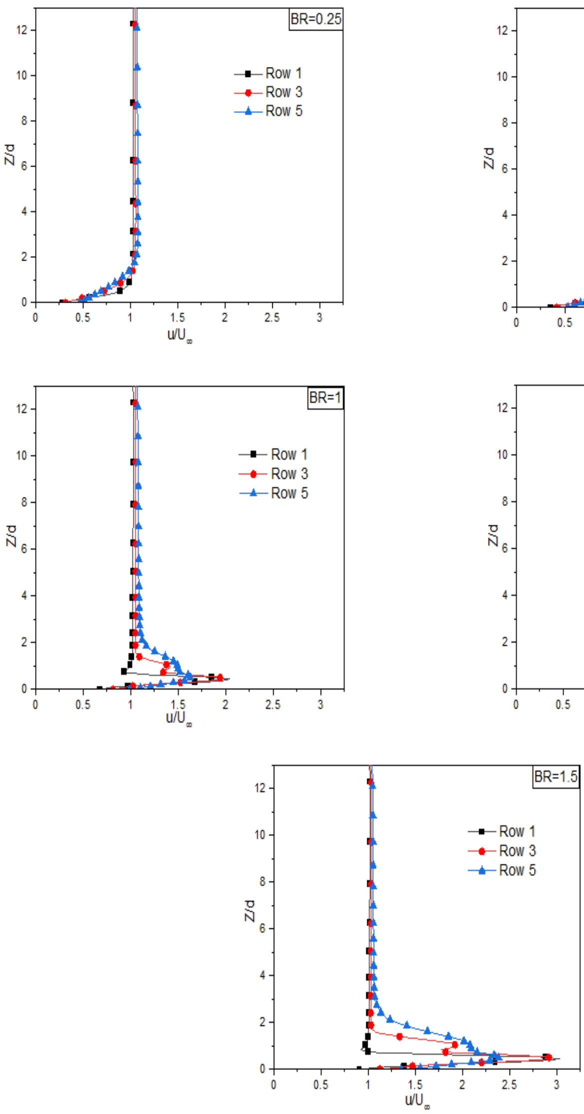

Fig.11 Velocity profiles downstream the effusion hole rows at different blowing ratios (α=30°)

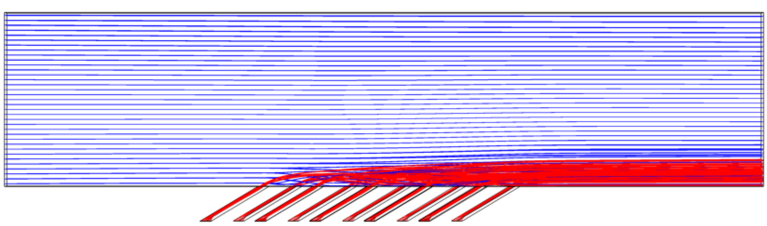

Fig.12 Velocity field streamlines along the solution domain for blowing ratio 1.5 at injection angle 30°

6.3 Temperature Boundary Profile

From the Fig. 13, it is observed for the row 1, the minimum penetration height is seen due to less interaction of coolant with the mainstream flow. Further in the downstream rows in streamwise direction at rows 3 and 5 the interaction between the fluid increases by interaction with the coolant flow from upstream rows together and this affects the flow field topology. From the Fig. 13 the kidney shaped counter rotating vortex pair is visible in each effusion holes and this flattens downstream in the streamwise direction due to addition of coolant flow coming from upstream holes. In the Fig.14 a coolant core formation is noticeable near the wall region Z/d>3 as the coolant is injected from the effusion holes. The variations in temperature boundary layer are seen in the region Z/d>3 and the outer portion Z/d<3 remains unchanged as of mainstream flow. It is interesting to note that the thermal boundary layer thickness increases as BR increases from 0.25 to 1.5.

6.4 Effect of Injection Angle (α) on Adiabatic Effectiveness

Simulations have been carried for different blowing ratios (BR) at injection angles (α) of 30^o and 60^o. The values of adiabatic effectiveness obtained at blowing ratio (BR) equal to 0.25 have been plotted in Fig. 15. Adiabatic effectiveness (η) is high at $\alpha=30^o$ as compared to that at $\alpha=60^o$. It is an account of the fact that at low values of injection angle the coolant flow stays for more intervals and has more interaction with the main flow as compared to that at high values of injection angles. This leads to higher values of convection heat transfer at low injection angles. Unlike this at $\alpha=60^o$ (i.e., at high value of injection), the coolant attaches to the surface with less interactions with the main flow. In the region (X_2), there is maximum difference in the peak values of adiabatic efficiency (η) as compared to that in the region (X_3). The reason being that in the region (X_2) there is more interaction with the main flow at lower values of injection angles.

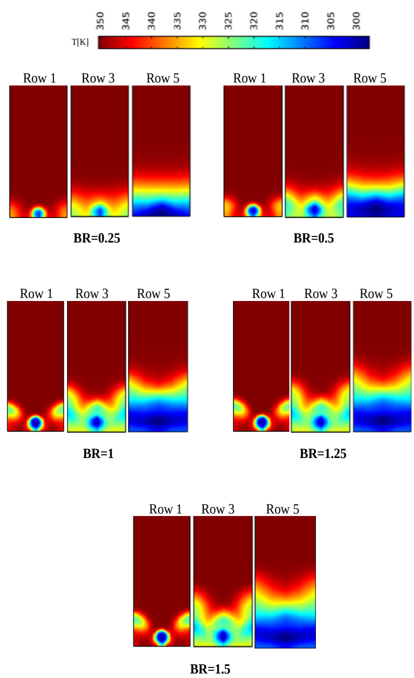

Fig. 13 Development of temperature fields on the YZ plane for different blowing ratios at α=30°

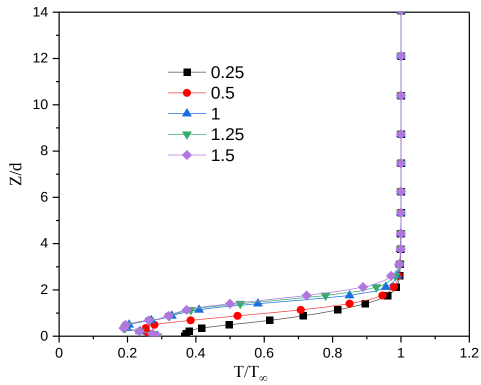

Fig. 14 Normalized Temperature boundary profiles at row 5 for α=30°

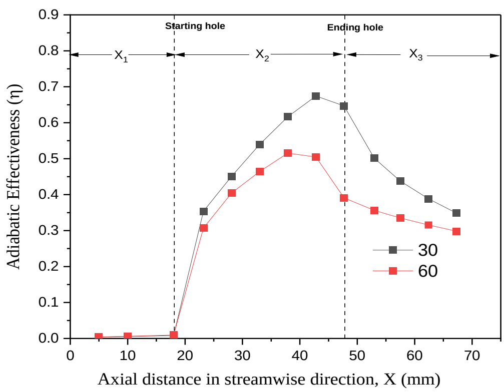

Fig. 15 Comparison of centerline adiabatic effectiveness at blowing ratio (BR) of 0.25 for different injection angles

6.5 Area-Averaged Adiabatic Effectiveness ($\bar{\eta}$)

The Fig. 16 shows the plot between the area-averaged adiabatic effectiveness ($\bar{\eta}$) at different BR in the regions X_2 and X_3. It is observed that in the region X_2, the $\bar{\eta}$ value is higher for low BR compared to high BR. The value of area-averaged adiabatic effectiveness ($\bar{\eta}$) is 0.49, 0.48, 0.47, 0.44 and 0.43 for blowing ratios 0.25, 0.5, 1.0, 1.25 and 1.5 respectively. But opposite behavior is observed in region X_3. The value of area-averaged adiabatic effectiveness ($\bar{\eta}$) is 0.44, 0.58, 0.70, 0.71 and 0.71 for blowing ratios 0.25, 0.5, 1.0, 1.25 and 1.5 respectively. For both injection angles 30^o and 60^o it is observed that the $\bar{\eta}$ increases with increase in BR. However, value of $\bar{\eta}$ for 30^o injection angle is more than of injection angle 60^o. For higher value of BR, the large amount of coolant mass flow is injected through effusion holes which increases the thermal film layer this provide and ensures proper protection for combustion liners in the combustion chamber.

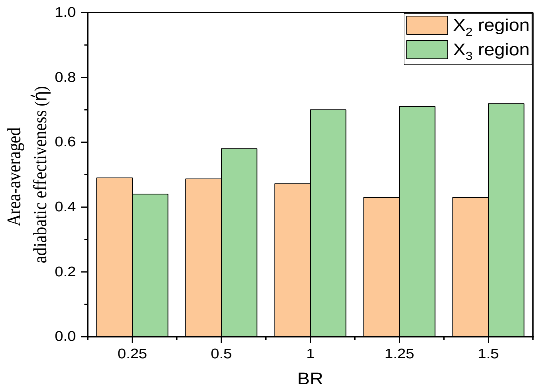

Fig. 16 Area-averaged adiabatic effectiveness ($\bar{\eta}$) with blowing ratio (BR) in the effusion region (X_2) and downstream region of effusion holes (X_3)

7. Conclusions

Computational investigations are carried to study the effect of blowing ratio (BR) and injection angle (α) on effusion cooling system of gas turbine combustor liners. The temperature and velocity profile shapes were obtained through simulation measured at different sections in streamwise direction for range of blowing ratios. The adiabatic effectiveness has been evaluated accordingly for all the cases.

The conclusions of the study are as follows:

- The adiabatic effectiveness is zero in the upstream region (X_1) as there is no coolant flow on the adiabatic surface.
- In the effusion region (X_2), the adiabatic effectiveness is high for low blowing ratios and the tendency decreases as the blowing ratio increases from 0.25 to 1.5. In the region (X_3) downstream of effusion region the value of adiabatic effectiveness is low for low blowing ratio and the value increases as the blowing ratio increases from 0.25 to 1.5.
- The adiabatic efficiency is more at injection angle of 30° as compared to that at injection angle of 60°.

Blowing ratio is a key parameter in the design aspect of effusion cooling system. The overall gas turbine efficiency will be impacted by the large need for coolant mass flow rate at high blowing ratios. For low blowing ratios, low coolant mass flow rate will not be enough to protect the liners. So, the selection of a blowing ratio for effusion system should be considered carefully to provide and ensure proper protection of combustion chamber.

Nomenclature

d	m	Diameter of effusion hole
t	m	Thickness of effusion plate
S_x/d	-	Streamwise distance between two adjacent holes in x-direction
S_y/d	-	Spanwise distance between two adjacent holes in y-direction
T	K	Temperature
U	m/s	Flow velocity
X	m	Streamwise coordinate
Y	m	Spanwise coordinate

Z	m	Normal coordinate
BR	-	Blowing ratio
DR	-	Density ratio
VR	-	Velocity Ratio
Greek letters		
α	°	Injection angle
η	-	Adiabatic effectiveness
$\bar{\eta}$	-	Area-averaged adiabatic effectiveness
ρ	kg/m^3	Density
Subscripts		
wt		Wall temperature on adiabatic surface of effusion plate
c		Coolant flow
∞		Mainstream flow

References

[1] Yuen CHN, Martinez-Botas RF. Film cooling characteristics of rows of round holes at various streamwise angles in a crossflow: Part I. Effectiveness. International Journal of Heat and Mass Transfer, 2005; 48(23-24), 4995-5016. https://doi.org/10.1016/j.ijheatmasstransfer.2005.05.019

[2] Qayoum, A, Panigrahi P. Experimental investigation of heat transfer enhancement in a two-pass square duct by permeable ribs. Heat Transfer Engineering, 2019; 40:8 640-651. https://doi.org/10.1080/01457632.2018.1436649

[3] Rasool A, Qayoum A. Numerical analysis of heat transfer and friction factor in two-pass channels with variable rib shapes. Journal homepage: http://iieta. org/Journals/IJHT, 2018; 36:1 40-48. https://doi.org/10.18280/ijht.360106

[4] Rasool A, Qayoum A. Numerical Investigation of Fluid Flow and Heat Transfer in a Two-Pass Channel with Perforated Ribs. Pertanika Journal of Science & Technology, 2018; 26:4.

[5] Röger M, Buck R, Müller-Steinhagen H. Numerical and experimental investigation of a multiple air jet cooling system for application in a solar thermal receiver, 2005; 863-876. https://doi.org/10.1115/1.1928910

[6] El-Gabry LA, Kaminski DA. Numerical investigation of jet impingement with cross flow-comparison of yang-shih and standard k-ϵ turbulence models. Numerical Heat Transfer, Part A, 2005; 47:5 441-469. https://doi.org/10.1080/10407780590891254

[7] Silieti M, Divo E, Kassab AJ. Numerical investigation of adiabatic and conjugate film cooling effectiveness on a single cylindrical film-cooling hole. In ASME International Mechanical Engineering Congress and Exposition, 2004; 4711: 333-343. https://doi.org/10.1115/IMECE2004-62196

[8] Baldauf S, Scheurlen M, Schulz A, Wittig S. Heat flux reduction from film cooling and correlation of heat transfer coefficients from thermographic measurements at engine like conditions. In Turbo Expo: Power for Land, Sea, and Air, 2002; 36088: 163-174. https://doi.org/10.1115/GT2002-30181

[9] Ligrani P, Goodro M, Fox M, Moon HK. Full-coverage film cooling: film effectiveness and heat transfer coefficients for dense and sparse hole arrays at different blowing ratios., ASME J. Turbomach.134, 2012; 061039. https://doi.org/10.1115/1.4006304

[10] Bohn D, Kusterer K. Blowing ratio influence on jet mixing flow phenomena at the leading edge. In 37th Aerospace Sciences Meeting and Exhibit, 1999; 670. https://doi.org/10.2514/6.1999-670

[11] Bailey JC, Intile J, Fric TF, Tolpadi AK, Nirmalan NV, Bunker RS. Experimental and numerical study of heat transfer in a gas turbine combustor liner. J. Eng. Gas Turbines Power, 2003; 125:4 994-1002. https://doi.org/10.1115/1.1615256

[12] Liu X, Zheng H. Influence of deflection hole angle on effusion cooling in a real combustion chamber condition. Thermal Science, 2015; 19:2 645-656. https://doi.org/10.2298/TSCI140107043L
[13] Andrews GE, Alikhanizadeh M, Tehrani FB, Hussain CI, Azari MK. (1988). Small diameter film cooling holes: the influence of hole size and pitch. International Journal of Turbo and Jet Engines, 1998; 5:1-4 61-72. https://doi.org/10.1515/TJJ.1988.5.1-4.61
[14] Andrews GE, Asere AA, Gupta ML, Mkpadi MC. Full coverage discrete hole film cooling: the influence of hole size. In Turbo Expo: Power for Land, Sea, and Air American Society of Mechanical Engineers, 1985; 79405: V003T09A003. https://doi.org/10.1115/85-GT-47
[15] Andrews GE, Gupta ML, Mkpadi, MC. Full coverage discrete hole wall cooling: Cooling effectiveness. In Turbo Expo: Power for Land, Sea, and Air American Society of Mechanical Engineers, 1984; 79498; V004T09A018. https://doi.org/10.1115/84-GT-212
[16] Lin Y, Song B, Li B, Liu G, Wu Z. (Investigation of film cooling effectiveness of full-coverage inclined multihole walls with different hole arrangements. In Turbo Expo: Power for Land, Sea, and Air, 2003; 36886: 651-660. https://doi.org/10.1115/GT2003-38881
[17] Zhang C, Lin Y, Xu Q, Liu G, Song B. Cooling effectiveness of effusion walls with deflection hole angles measured by infrared imaging. Applied thermal engineering, 2009; 29:5-6 966-972. https://doi.org/10.1016/j.applthermaleng.2008.05.011
[18] Leger B, Miron P, Emidio JM. Geometric and aero-thermal influences on multiholed plate temperature: application on combustor wall. International Journal of Heat and Mass Transfer, 2003; 46:7 1215-1222. https://doi.org/10.1016/S0017-9310(02)00396-4
[19] Gustafsson KB. Experimental studies of effusion cooling. Chalmers University of Technology, 2001.
[20] Sasaki M, Takahara K, Kumagai T, Hamano M. Film cooling effectiveness for injection from multirow holes, J. Eng. Power 101, 1979; 101-108. https://doi.org/10.1115/1.3446430
[21] Cerri G, Giovannelli A, Battisti L, Fedrizzi R. Advances in effusive cooling techniques of gas turbines. Applied Thermal Engineering, 2007; 27:4 692-698. https://doi.org/10.1016/j.applthermaleng.2006.10.012
[22] Kumar KY, Qayoum A, Saleem, S, Qayoum F. Effusion Cooling In Gas Turbine Combustion Chambers-A Comprehensive Review. In IOP Conference Series: Materials Science and Engineering, 2020; 804:1 012003. https://doi.org/10.1088/1757-899X/804/1/012003
[23] Scrittore JJ, Thole KA, Burd SW. Investigation of velocity profiles for effusion cooling of a combustor liner, Journal of Turbomachinery.129, 2007; 518-526. https://doi.org/10.1115/1.2720492
[24] Pietrzyk JR, Bogard DG, Crawford ME. Hydrodynamic measurements of jets in crossflow for gas turbine film cooling applications, J. Turbomach 111, 1989; 139-145. https://doi.org/10.1115/1.3262248